Regenerative Therapy 22 (2023) 99–108

Contents lists available at ScienceDirect

Regenerative Therapy

journal homepage: http://www.elsevier.com/locate/reth

Original Article

Introduction of tenomodulin by gene transfection vectors for rat bone tissue regeneration

Han Wang [a], Taichi Tenkumo [a, *], Eiji Nemoto [b], Yoshiaki Kanda [a], Toru Ogawa [a], Keiichi Sasaki [a]

[a] Division of Advanced Prosthetic Dentistry, Tohoku University Graduate School of Dentistry, 4-1 Seiryo-machi, Aoba-ku, Sendai, 980-8575, Japan
[b] Division of Periodontology, Department of Oral Biology, Tohoku University Graduate School of Dentistry, 4-1 Seiryo-machi, Aoba-ku, Sendai, 980-8575, Japan

ARTICLE INFO

Article history:
Received 11 October 2022
Received in revised form
17 December 2022
Accepted 22 December 2022

Keywords:
Tenomodulin
Hard tissue formation
Gene transfection
Calcium phosphate
Cationic polymer

ABSTRACT

Introduction: Periodontal ligament is regenerated in association with hard tissue regeneration. Tenomodulin (Tnmd) expression has been confirmed in periodontal ligament and it reportedly inhibits angiogenesis or is involved in collagen fibril maturation. The introduction of Tnmd by gene transfection in bone tissue regeneration therapy might inhibit topical hard tissue formation and induce the formation of dense fibrous tissue. Therefore, the effect of Tnmd introduction by gene transfection technique in vitro and in vivo was investigated in this study.
Methods: Osteogenesis- and chondrogenesis-related gene expression levels in osteoblastic cells (MC3T3E1) and rat bone marrow derived cells were detected using qPCR three days after gene transfection with plasmid DNA (Tnmd) using non-viral gene transfection vectors: a calcium phosphate-based gene transfection vector (CaP(Tnmd)) or a cationic polymer-based reagent (JetPEI (Tnmd)). Next, an atelocollagen scaffold with or without CaP (Tnmd) or JetPEI (Tnmd) was implanted into a rat calvaria bone defect, and the remaining bone defect volume and the tissue reaction at 28 days after surgery were evaluated.
Results: Runx 2 and SP7 mRNA was reduced by JetPEI (Tnmd) in both cells, but not in CaP(Tnmd). The volume of expressed Tnmd was at 9 ng/mL in both gene transfection vector. The remaining bone defect volume of JetPEI (Tnmd) was significantly bigger than that of the other groups and CaP (EGFP), and that of CaP (Tnmd) was significantly bigger than that of CaP (EGFP).
Conclusions: Tnmd introduction treatment inhibits bone formation in artificial bone defect, however, the effect of that was dependent on non-viral gene transfection vector.

1. Introduction

Periodontitis is a lifestyle-related disease that causes the loss of alveolar bone or periodontal ligament, resulting in tooth loss. Periodontal tissue is a composite tissue and composed of gingiva, cementum, bone, and periodontal ligaments. Numerous scaffolds have been developed and applied with or without growth factors for bone regeneration in periodontal therapy [1]. On the other hand, periodontal ligaments support the chewing function as a ligament because the end of the collagen fiber is embedded in the cementum and the other side is embedded in the bone [2,3]. However, a method for the regeneration of functional periodontal ligament has not been established, and the regeneration is observed to be associated with bone regeneration. The periodontal ligament is often not regenerated, and ankylosis has been observed on a part of the tooth surface after periodontal regeneration therapy [4,5]. The consequences of ankylosis include progressive resorption of the root with bone replacement [6]. Thus, the prevention of ankylosis and the re-formation of functional periodontal ligaments are important for periodontal tissue regeneration therapy at the same time the new bone is formed. The localized introduction of an inhibitory factor of bone formation around the root surface is an attractive approach for periodontal ligament regeneration while performing bone regeneration in the vicinity.

Tenomodulin (Tnmd) is expressed in dense fibrous connective tissues, such as cornea, tendon, and ligaments, including

Abbreviations: CaP, calcium phosphate; rBMDCs, rat bone marrow-derived cells; Tnmd, tenomodulin; ELISA, enzyme-linked immunosorbent assay; FBS, fetal bovine serum.

* Corresponding author. Fax.: (+81)(022)717-8371.
E-mail address: taichi.tenkumo.a3@tohoku.ac.jp (T. Tenkumo).

Peer review under responsibility of the Japanese Society for Regenerative Medicine.

https://doi.org/10.1016/j.reth.2022.12.008

periodontal ligament, [7–11]. It is reported that Tnmd inhibits angiogenesis or is involved in collagen fibril maturation or proliferation [8,12–15]. Angiogenesis is associated with bone regeneration [16], and the osteogenic and chondrogenic differentiation of bone marrow-derived and adipose-derived stem cells obtained from mice overexpressing Tnmd was significantly reduced [15]. Ectopic bone formation was observed in intervertebral discs in Tnmd knockout mice [17]. Therefore, a topical application of Tnmd might induce the formation of dense fibrous tissues and prevent ankylosis by leading to the coordinated regeneration of bone. However, Tnmd is a type II transmembrane glycoprotein and cannot be applied to a cell or topical tissue as a solution, similar to released proteins, such as BMP-2 or FGF-2. For application of Tnmd in tissue regeneration therapy, the gene transfection technique is a suitable method.

We have developed a non-viral gene transfection vector based on calcium phosphate (CaP) nanoparticles, with an improved gene transfection efficiency [18,19] and demonstrated that successful growth factor release resulted in gene transfection with a collagen scaffold in a bone defect model [20]. In this study, Tnmd was introduced by non-viral gene transfection vectors: a CaP-based gene transfection vector and a cationic polymer-based reagent (JetPEI) and their effect in mouse precursor osteoblast-like cells (MC3T3E1) and rat bone marrow derived cells and tissue reaction in a cranium bone defect model after Tnmd introduction were investigated.

2. Methods

2.1. Preparation of gene transfection vectors

CaP nanoparticles and a cationic polymer-based reagent (JetPEI® or in vivo-JetPEI™; Polyplus, Shanghai, China) were used as non-viral gene transfection vectors in this study. CaP nanoparticles were prepared according to a previously reported method [20]. Briefly, the core of the CaP nanoparticles was fabricated by mixing an aqueous solution of calcium nitrate (18 mM, pH 9.0, Wako, Tokyo, Japan) and an equal volume of an aqueous solution of diammonium hydrogen phosphate (10.8 mM, pH 9.0, Wako, Tokyo, Japan) using a peristaltic pump. Then, 18 μL of the prepared CaP dispersion was immediately mixed with 7.3 μL of aqueous plasmid DNA solution, that is, pcDNA3.1+C-HA -Tenomodulin (1 mg/mL, GeneScript, Japan) or pUC57-EGFP (enhanced green fluorescent protein; 1 mg/mL, GeneScript, Japan) for gene expression analysis and animal experiments or pcDNA3.1 (+)-C-HA mCherry (1 mg/mL, GeneScript, Japan) for gene transfection efficiency tests. After mixing, calcium nitrate (18 mM, pH 9.0; 9 μL) and diammonium hydrogen phosphate (10.8 mM, pH 9.0; 9 μL, Wako) solutions were added to the prepared dispersion and mixed to cover the CaP core loading the plasmid DNA. Finally, an aqueous solution of protamine sulfate (10 mg/mL; 7.3 μL, Wako, Japan) was added to prepare the CaP nanoparticles. The obtained nanoparticle dispersion was centrifuged at 16,099×*g* at 4 °C for 10 min to remove excess plasmid DNA or protamine from the prepared CaP nanoparticles. After the supernatant was removed, CaP nanoparticles were redispersed into 25 μL of fresh distilled water and denoted as CaP (Tnmd), CaP (EGFP), and CaP (mCherry), respectively. EGFP has no osteoinductivity; hence, it was used as a control. The structure of these CaP nanoparticles is demonstrated in our previous reports [20,21]. For the fabrication of a cationic polymer-based reagent, JetPEI was used according to the manufacturer's protocol. Briefly, 0.5 μg of an aqueous solution of pcDNA3.1+C-HA-Tenomodulin (1 mg/mL), 0.5 μg of an aqueous solution of pcDNA3.1 (+)-C-HA mCherry or 1 μL of JetPEI reagent was mixed with 24.5 or 24 μL of NaCl (150 mM), respectively. The obtained 25 μL of JetPEI solution was added to 25 μL of the DNA solution. After incubation for 20 min at room temperature (20–27 °C), the reacted solution was denoted as JetPEI (Tnmd) or JetPEI (mCherry).

For animal experiments, an aqueous solution of pcDNA3.1+ C-HA-Tenomodulin (1 mg/mL) was mixed with 10% glucose solution. Next, in vivo JetPEI was mixed with 10% glucose solution. The obtained in vivo JetPEI solution was added to DNA solution and incubated for 15 min at 20–27 °C.

In gene transfer experiments using animals, the mixing ratio for all applied solutions in the protocol was the same, but the volume of each solution was different. The volume of plasmid DNA attached to CaP nanoparticles was calculated by measuring the volume of the remaining plasmid DNA in the supernatant by UV microvolume spectroscopy (Nanodrop 2000; Thermo Scientific, Tokyo, Japan). The volume of protamine attached to the CaP nanoparticles was also calculated by UV using a Protein Assay BCA kit (Nacalai Tesque, Kyoto, Japan) according to the manufacturer's protocol as in the DNA measurement. The volume of CaP nanoparticles applied in the cell or scaffold was calculated as described in a previous report [20,22] and as shown in Table 1.

2.2. Animals

The study was carried out in compliance with the ARRIVE guidelines. All animals used in this experiment were handled according to the Guide for the Care and Use of Laboratory Animals of Tohoku University, Japan. Animals were obtained from Japan SLC Inc (Shizuoka, Japan). All animal experimental protocols were reviewed and approved by the Institutional Animal Experiment Committee of Tohoku University (2020 DnA-026-01).

2.3. Cell culture

MC3T3E1 cells were obtained from the RIKEN Cell Bank (Tsukuba, Japan). Cells were cultured in alpha-modified Eagle's medium (α-MEM; Nacalai Tesque, Kyoto, Japan) supplemented with 10% fetal bovine serum (FBS) (Thermo Fisher Scientific, Tokyo, Japan), 100 U/mL penicillin, and 100 U/mL streptomycin (Nacalai Tesque, Kyoto, Japan) at 37 °C in the presence of 5% CO_2. To collect the rat bone marrow-derived cells (rBMDCs), five rats (Jcl:Wistar, male, 8 week-old, 180–210 g) were sacrificed by overdose of sodium pentobarbital. Rat femur bones were extracted under general anesthesia and immediately immersed in PBS. The ends of the extracted femur bone were cut, and the bone marrow was collected using a needle and rinsed with PBS. The collected bone marrow was centrifuged at 800×*g* for 10 min to remove red blood cells and debris. After re-suspension with α-MEM, the cells were seeded in 10 cm tissue culture dishes with α-MEM containing 10% FBS, 100 U/mL penicillin, and 100 U/mL streptomycin at 37 °C in the presence of 5% CO_2. These cells were denoted as rBMDCs. Passage 2–5 cells were used.

2.4. Gene transfection efficiency

MC3T3E1 cells and rBMDCs were seeded in 48-well plates at a density of 1×10^4 per well, in the conditions described above. Next, 24 h later, the medium was removed, and 225 or 200 μL of fresh culture medium supplemented and 25 μL of CaP (mCherry) or 50 μL of JetPEI (mCherry) solutions were added to the cells, respectively. After 12 h, the transfection efficiency was calculated based on the ratio of fluorescing cells (mCherry-expressing cells resulting from successful gene transfection) to the total number of examined cells by using transmission light microscopy and fluorescence microscopy (magnification × 200; BZ-9000; Keyence). The value at no autofluorescence in an untransfected cell was used as a threshold

Table 1
Concentrations of calcium phosphate nanoparticles loaded with pcDNA3.1+C-HA−Tenomodulin, pUC57-EGFP and pcDNA3.1 (+)-C-HA mCherry.

Concentration (μg/well in 48-well plates)	CaP	pcDNA3.1+C-HA−Tenomodulin	pUC57-EGFP	pcDNA3.1 (+)-C-HA mCherry	Protamine
JetPEI (Tnmd)	0	0.5	0	0	0
CaP (Tnmd)	5.1	1.6	0	0	3.0
CaP (EGFP)	5.1	0	1.6	0	2.8
JetPEI (mCherry)	0	0	0	0.5	0
CaP (mCherry)	5.1	0	0	1.6	2.8
Untransfected cells	0	0	0	0	0
For animal experiments (μg/scaffold)	CaP	pcDNA3.1+C-HA−Tenomodulin	pUC57-EGFP	pcDNA3.1 (+)-C-HA mCherry	Protamine
Scaffold alone	0	0	0	0	0
JetPEI (Tnmd)	0	7	0	0	0
CaP (Tnmd)	23.0	7.3	0	0	11.2
CaP (EGFP)	23.0	0	7.3	0	10.7

(exposure time: 4.0 s). Dead cells (as recognized by their shapes) were not included in the computation process.

2.5. Enzyme-linked immunosorbent assay (ELISA) and calcium concentration analysis

MC3T3E1 cells and rBMDCs were respectively seeded in 48-well plates at a density of 2×10^4 cells per well under the conditions described above. The supernatant was collected at 3 days after transfection. To determine alkaline phosphatase activity in the supernatant, the absorbance of the reaction mixture was measured at 405 nm with Labo Assay ALP (Fujifilm Wako, Tokyo, Japan), according to the manufacturer's instructions, using a microplate reader (iMarktm microplate reader; Bio-Rad, Osaka, Japan).

To determine the calcium concentration in the supernatant, the absorbance of the reaction mixture was measured at 620 nm using the Calcium E-test Wako (Wako, Tokyo, Japan) according to the manufacturer's instructions. The calcium concentration was determined using the culture medium for normalization.

To determine the protein expression levels of Tnmd resulting from gene transfection, the cultured cells were dissolved in RIPA Lysis Buffer solution with Protease inhibitor cocktail and 1% SDS (Nacalai Tesque, Kyoto, Japan) (400 μL), according to the manufacturer's instructions. The reaction solution was collected and centrifugated at 16,099 g for 10 min. The supernatant was collected and subjected to ELISA for quantifying Tnmd (Rat Tnmd ELISA Kit from Wuhan Fine Biotech Co., Ltd, Biocompare, China). The absorbance of the reaction mixture was measured at 450 nm, according to the manufacturer's instructions, using a microplate reader (Spectra MAX 190, Molecular Devices, Japan).

2.6. Gene expression analysis

MC3T3E1 cells and rBMDCs were respectively seeded in 48-well plates at a density of 2×10^4 cells per well under the conditions described above. Approximately 24 h later, the medium was replaced with 250 μL fresh medium with ascorbic acid, and the prepared gene transfection vectors were added to the cells, as shown in Table 1. After 3 days, the cultured media were removed, and total RNA was collected using Cell Lysis RT-qPCR kits (Bio-Rad, Osaka, Japan). After the concentration of the obtained RNA was measured using UV microvolume spectroscopy (Nanodrop 2000), RNA (500 ng) was converted into cDNA using the iScript Advanced cDNA Synthesis Kit for RT-qPCR (Bio-Rad, Osaka, Japan). Next, 10 μL of SsoAdvanced Universal SYBR Green system (Bio-Rad Laboratories), 4 or 7 μL of DNase-free water, 2 μL of cDNA, and 2 or 1 μL of each primer were mixed, followed by polymerase activation and DNA denaturation at 95 °C for 30 s, followed by amplification for 40 cycles (denaturation at 95 °C for 10 s and annealing/extension at 60 °C for 30 s) using CFX96 (Bio-Rad, Osaka, Japan). The mRNA expression level of each target gene was determined using GAPDH as the control for normalization, using the △△CT method. The primer sequences for osteogenic and chondrogenic markers are shown in Table 2. The primers were purchased from Bio-Rad (Osaka, Japan) or FASMAC (Kanagawa, Japan). Each experiment was independently carried out over five times.

2.7. Animal experiments

2.7.1. CaP/collagen or in vivo JetPEI/collagen scaffold preparation

The pcDNA3.1+C-HA -Tenomodulin or pUC57-EGFP loading CaP or pcDNA3.1+C-HA −Tenomodulin loading in vivo-JetPEI dispersion was prepared as described in Section 2.1. The dose of each CaP nanoparticle or in vivo-JetPEI with loading plasmid DNA in the scaffolds is shown in Table 1. The bovine-derived atelocollagen sponge (diameter, 5 mm; Atelocollagen sponge MIGHTY, Koken, Tokyo, Japan) was cut at a height of 1.5 mm using a scalpel knife. Thereafter, 10 μL of each CaP dispersion was injected into the cut collagen sponge, freeze-dried, stored at −80 °C, and donated as CaP(Tnmd) or CaP(EGFP). Then, 56 μL of the in vivo-JetPEI dispersion was injected into cut collagen sponge within 30 min before the implantation into the rat and denoted as JetPEI (Tnmd).

Table 2
Sequences of gene-specific primers used for qPCR analysis.

Gene name		For rat bone marrow-derived cells Primer sequence 5′-3′	For MC3T3E1 Primer sequence 5′-3′
GAPDH	Fwd	GGCAAGTTCAACGGCACAG	GACTTCAACAGCAACTCCCAC
	Rev	CGCCAGTAGACTCCACGAC	TCCACCACCCTGTTGCTGTA
ALP	PrimePCR™ SYBR® Green Assay: Alpp, Rat		PrimePCR™ SYBR® Green Assay: Alpl, Mouse
OCN	PrimePCR™ SYBR® Green Assay: Bglap, Rat		PrimePCR™ SYBR® Green Assay: Bglap, Mouse
Runx 2	PrimePCR™ SYBR® Green Assay: Runx 2, Rat		PrimePCR™ SYBR® Green Assay: Runx 2, Mouse
SP7	PrimePCR™ SYBR® Green Assay: Sp7, Rat		PrimePCR™ SYBR® Green Assay: Sp7, Mouse
Col2a	PrimePCR™ SYBR® Green Assay: Col2a1, Rat		PrimePCR™ SYBR® Green Assay: Col2a1, Mouse
SOX9	PrimePCR™ SYBR® Green Assay: Sox 9, Rat		PrimePCR™ SYBR® Green Assay: Sox 9, Mouse

2.7.2. Surgical procedures

Twenty rats (Jcl:Wistar, male, 8 week-old, 180–220 g) were anesthetized with an intraperitoneal injection of medetomidine (Domitor, 0.375 mg/kg body weight; pon Zenyaku Kogyo, Japan) and midazolam (Sandoz, 2 mg/kg body weight; Meiji Seika Co., Tokyo, Japan), followed by lidocaine hydrochloride with 2% Epinephrine (0.1 mL, Sandoz, Meiji Seika Co., Tokyo, Japan) in local. After shaving the head, the flaps and periosteum were revealed. Two circular osseous defects (diameter, 5 mm) were prepared on the cranium using a trephine bur with an external diameter of 5 mm, which was operated at 8000 rpm with sterile saline irrigation, using a dental electric motor system (VIVAace; NSK, Kanuma, Japan). The prepared scaffolds were then implanted into the prepared defects. After implantation, the flap was rigidly sutured with non-absorbable 4-0 silk sutures (Mani, Tochigi, Japan) to prevent infection and loss of scaffolds. Rats were sacrificed by subjecting them to an overdose of sodium pentobarbital at 28 days after surgery, and the crania, including the implants, were extracted, and immediately immersed in PBS.

2.7.3. Micro-CT evaluation of bone defects

All extracted samples were scanned using microcomputed tomography (ScanXmate-E090; X-ray tube potential = 60 kVp, current = 80 μA, integration time = 1000 ms, number of projections = 600/360°, isotropic nominal voxel sizes of 50 μm; Comscan Tecno Co. Ltd., Kanagawa, Japan). The volumetric tissue mineral density (TMD) of newly formed hard tissues was measured at 3000 × 3000 × 2000 μm inside the scaffold using a 3D structural analysis (TRI/3D-VEI; Ra-toc System Engineering Co. Ltd., Tokyo, Japan). The remaining bone defect volume was measured using ImageJ (National Institutes of Health, Bethesda, MD, USA). The sample number of all groups was ten, as 40 holes were formed in twenty rats.

2.7.4. Biochemical evaluation

After micro-CT analysis, five samples in each group were used for determination of Tnmd expression. The implanted area (diameter 5 mm) was extracted using a trephine bur with an external diameter of 5 mm, operated at 10000 rpm with sterile saline irrigation, using a dental electric motor system (VIVAace, NSK, Kanuma, Japan). The extracted tissues were crushed using a multi-bead-shocker MB2000 (3000 rpm, 10 s; 1 cycle; YASUI KIKAI, Japan). The crushed tissue was dissolved in RIPA Lysis Buffer solution (1000 μL; Nacalai, Kyoto, Japan) and homogenized via ultrasonic treatment for 10 s, followed by centrifugation at 16,099×*g* for 15 min, according to the manufacturer's protocol. The supernatant was subjected to ELISA for quantifying Tnmd (Rat Tnmd ELISA Kit from Wuhan Fine Biotech Co., Ltd, Biocompare, China). The absorbance of the reaction mixture was measured at 450 nm, according to the manufacturer's instructions, using a microplate reader (Spectra MAX 190, Molecular Devices, Japan).

2.7.5. Histological and immunohistochemistry analysis

After micro-CT analysis, five samples in each group were used for histological analysis. After fixing with 4% glutaraldehyde for 1 day, the samples were decalcified in 17.7% EDTA (OSTEOSOFT, Merck Millipore, Tokyo, Japan). The samples were dehydrated in an ascending series of ethanol solutions and embedded in paraffin. The tissue sections (6-μm thick) were stained with hematoxylin and eosin (H&E), Toluidine Blue (0.05%Toluidine Blue Solution (pH4.1), Fujifilm Wako, Japan), and Elastica Masson. Histology was examined under a light microscope. To evaluate Tnmd expression, sliced sections were stained with a Tnmd polyclonal antibody (rabbit-poly (anti-Tnmd), diluted 1:2000 in PBS; Bioss, USA). All cells and Tnmd-positive cells were counted in an area of 700 μm × 530 μm in three stained sections at the center of the scaffold, and the ratio of Tnmd-positive cells to all cells in 371,000 μm^2 was calculated.

2.8. Statistical analysis

All data are expressed as mean ± standard deviation (SD). First, normal data distribution was verified using the Shapiro–Wilk test, and differences were assessed by one-way analysis of variance or the multiple comparison test. For multiple comparison test, statistical differences between groups in normally distributed data were assessed by the post-hoc–Tukey Kramer HSD multiple comparison test and those in non-normal distribution data were assessed using the Dann–Bonferroni test. Statistical analyses were performed using SPSS 22.0 software (IBM, Tokyo, Japan). Differences were considered significant at $p < 0.05$.

3. Results

3.1. Effect of treatment with gene transfection vector loaded with plasmid DNA (Tnmd) in MC3T3E1 cells and rBMDCs

The gene transfection efficiency of CaP (mCherry) was statistically at the same level as that of JetPEI (mCherry) (Fig. 1A and B). Fig. 1C and D shows the protein level of Tnmd resulting from gene transfection in MC3T3E1 cells and rBMDCs; levels in the CaP (Tnmd) and JetPEI (Tnmd) groups were significantly higher than those in the other groups ($p < 0.05$). There was no significant difference in the expression levels between CaP (Tnmd) and JetPEI (Tnmd).

Fig. 2 shows the gene expression level in MC3T3E1 cells at 3 days after Tnmd expression by gene transfection. The gene expression levels of Runx 2, SP7, and SOX9 in the JetPEI (Tnmd) group were significantly lower than those in untransfected cells ($p < 0.05$). Conversely, there was no significant difference in the expression level of all genes, except SP7, in the CaP (Tnmd) group compared to those in the untransfected cell group, while levels of SP7 in the CaP (Tnmd) group were lower that in the CaP (EGFP) group ($p < 0.05$). The gene expression levels of ALP and Col2a in the CaP(EGFP) group were significantly higher than those in untransfected cells ($p < 0.05$). Fig. 3 shows the gene expression levels in rBMDCs at 3 days after Tnmd expression by gene transfection. The gene expression levels of ALP, Runx2, and SP7 in the JetPEI (Tnmd) group were significantly lower than those in untransfected cells ($p < 0.05$). The gene expression level of SP7 in the CaP (Tnmd) group was lower than that in untransfected cells, while that of ALP in the CaP (Tnmd) group were lower than those in the CaP (EGFP) group ($p < 0.05$).

The volume of released ALP in the supernatant of CaP-transfected MC3T3E1 cells and rBMDCs was significantly higher than that in untransfected cells (Fig. 4A and B). There were no significant differences between the values for JetPEI-transfected cells and untransfected cells. The calcium ion concentration in the supernatant of CaP (Tnmd)- and CaP (EGFP)-transfected cells was significantly higher than that of the others in both cell lines (Fig. 4C and D) ($p < 0.05$).

3.2. Tissue reactions of the topical gene transfection with plasmid DNA (Tnmd) in collagen scaffold in the rat cranium bone defect

Table 3 shows the ratio of Tnmd-positive cells at 28 days after implantation of collagen scaffolds, including plasmid DNA (Tnmd)-

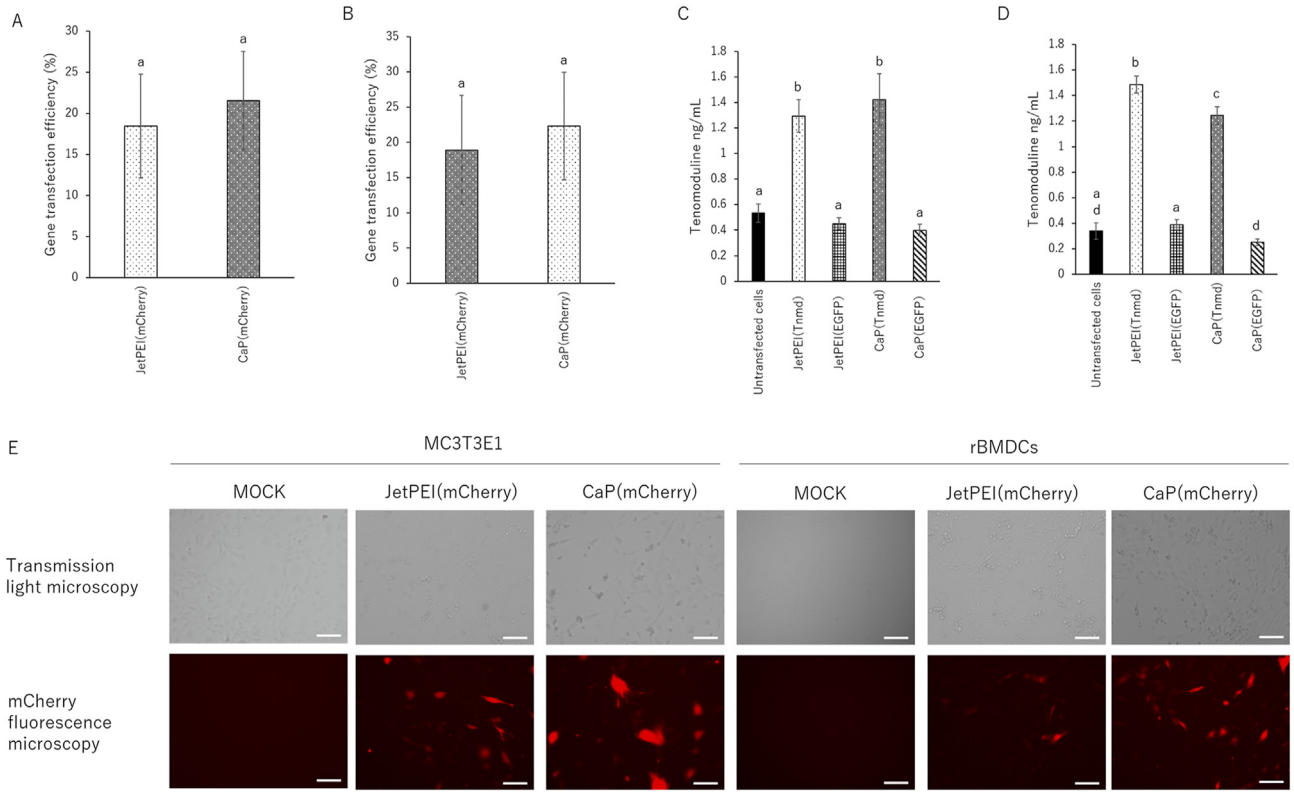

Fig. 1. Transfection efficiency of (A) MC3T3E1 and (B) rat bone marrow-derived cells (rBMDCs). Determination of Tnmd expression level 3 days after gene transfection in MC3T3E1 cells (C) and rBMDCs (D). Values and error bars indicate the mean and standard deviation, respectively. Significant differences ($p < 0.05$) between groups are denoted by different superscript letters (i.e., bars with the same letter are not significantly different) (E) Transmission light microscopy (TLM) and fluorescence microscopy (FM) of transfected cells. Representative images of MC3T3E1 and rBMDC 12 h after CaP (EGFP) or JetPEI (EGFP) application. Transfected cells appear green under fluorescence microscopy. Magnification: ×20. Bar = 100 μm.

loaded CaP nanoparticles or JetPEI in the cranium bone defect. The numbers of Tnmd-stained cells of the CaP (Tnmd) and JetPEI (Tnmd) groups were significantly higher than those of the CaP (EGFP) and scaffold alone groups ($p < 0.05$).

Fig. 5 shows the histological or immunohistochemical images of all groups at 28 days after implantation. No infection, severe inflammation, necrosis, or drainage was observed in any group. Newly formed hard tissue was observed around collagen fibers in all groups, and osteocyte-like cells were observed inside the newly formed hard tissues (Fig. 5A and B). The formed new hard tissue was stained as a purplish red or blue-green spot by Elastica Masson stain (Fig. 5D) and as a blue and bluish-purple spot by toluidine blue stain (Fig. 5E). Using the Elastica Masson stain, a blue-green stained fiber was abundantly observed in the JetPEI (Tnmd) and Cap (Tnmd) groups compared to that in the scaffold alone and CaP (EGFP) groups; however, the fiber direction was haphazard. The elastic fiber (black-stained area) was not observed in the Tnmd expression groups. The remaining collagen fiber of the scaffold stained red in the Elastica Masson staining (Fig. 5C and D) and light blue in the toluidine blue staining (Fig. 5E) and was observed in all groups. The brown cell in Fig. 5F shows Tnmd-stained cells, and positive cells were observed in and outside of the scaffold in all groups (see Fig. 5).

Fig. 6A shows the expression of Tnmd in the scaffold. Tnmd concentrations in the CaP (Tnmd) and JetPEI (Tnmd) groups in the scaffold were 9.2 ± 1.0 and 9.5 ± 0.9 ng/mL/scaffold, respectively and significantly higher than those in the CaP (EGFP) (2.6 ± 1.0 ng/mL/scaffold) and scaffold alone (2.2 ± 0.1 ng/mL/scaffold) groups ($p < 0.05$). There was no significant difference between CaP (Tnmd) and JetPEI (Tnmd). The results of micro-computed tomography analysis are shown in Fig. 6B, C, and D. The remaining bone defect volume of JetPEI (Tnmd) was significantly bigger than that of the other groups ($p < 0.05$), and that of CaP (Tnmd) was significantly bigger than that of the CaP (EGFP) ($p < 0.05$) (Fig. 6B). The tissue mineral density of the CaP (Tnmd) group was 980 ± 217 mg/cm3, which was significantly higher than that of the JetPEI (Tnmd) (252 ± 162 mg/cm3) and scaffold alone (293 ± 207 mg/cm3) groups, with no significant difference compared to that of the CaP (EGFP) group (702 ± 137 mg/cm3) (Fig. 6C and D) shows the micro-computed tomography images of each sample.

4. Discussion

Gene transfection vectors are mainly classified into two groups: viral vectors and non-viral vectors. Viral vectors have a high gene transfection efficiency, but their risk of cytotoxicity [23], immunogenicity [24], and potential recombination or complementation [25] cannot be denied. By contrast, non-viral vectors are not associated with the above risks, even though they generally have a low gene transfection efficiency compared to viral vectors. An ideal gene transfection vector has high transfection efficiency and safety; especially, it should not cause canceration or mixing of proliferative viral particles during tissue regeneration therapy by the direct application. This is because cell-like proliferation, differentiation, or intercell interaction is high in the area of tissue regeneration or repair reaction. Among non-viral transfection vectors, Calcium phosphate has a high compatibility with protein, peptide, and plasmid DNA and is reported to be a carrier of DNA, albeit having a low transfection efficiency [26]. However, the transfection efficiency was improved by changing its size into a nano size and by

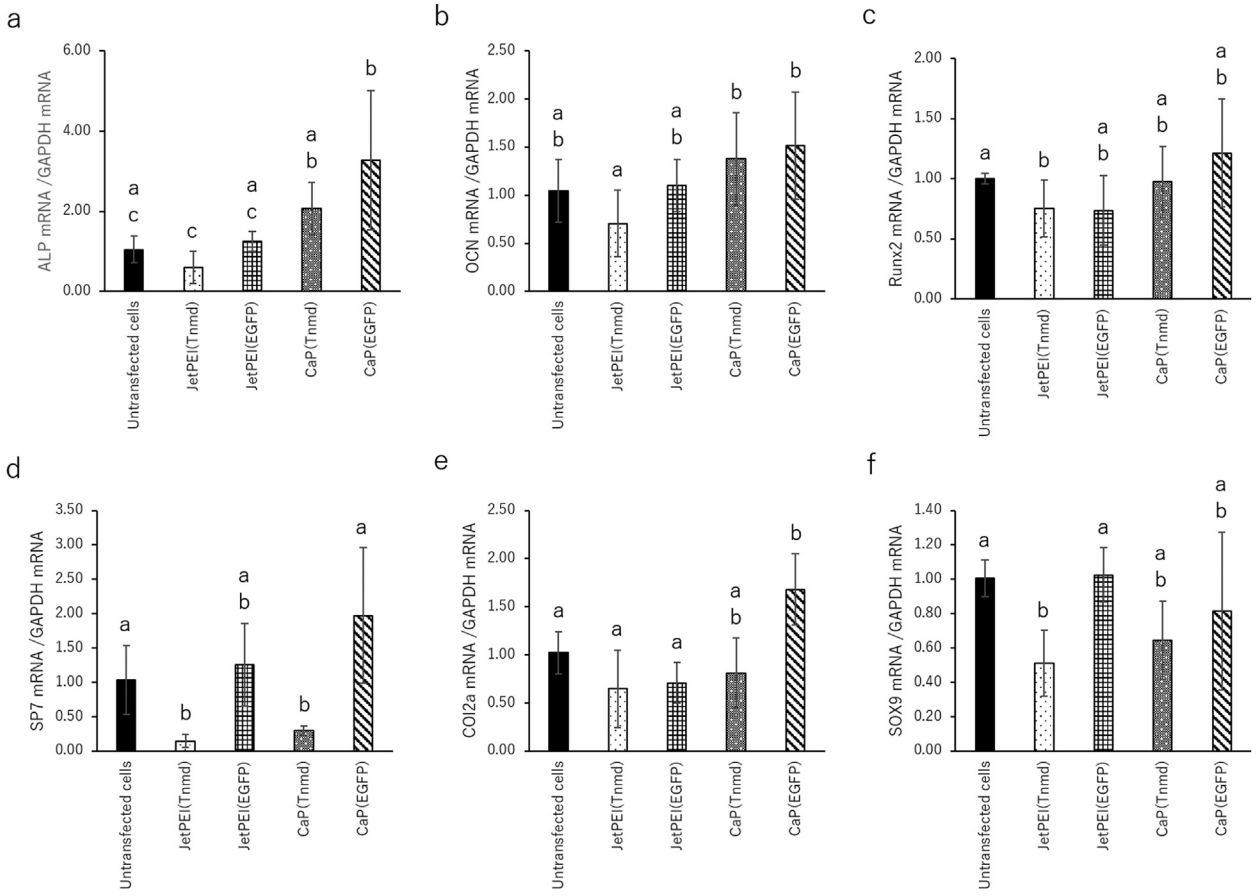

Fig. 2. Gene expression analyses in MC3T3E1 cells 3 days after gene transfection. (a) ALP mRNA expression, (b) OCN mRNA expression, (c) Runx 2 mRNA expression, (d) SP7 mRNA expression, (e) Col2αmRNA expression, and (f) SOX9 mRNA expression. Values and error bars indicate the mean and standard deviation, respectively. Significant differences ($p < 0.05$) between groups are denoted by different superscript letters (i.e., bars with the same letter are not significantly different).

protecting the DNA with a multi-shell structure [18,19]. Calcium and phosphate are the main component of bone, and numerous scaffolds based on calcium phosphate have been applied in bone tissue regeneration therapy [1,3]. Therefore, non-viral gene transfection vectors were used in this study.

The amount of mCherry and Tnmd expressed due to the gene transfection by CaP nanoparticles was similar to that of the polyethylenimine derivative reagent JetPEI, which is a commercially available non-viral gene transfection vector, confirming that the gene transfection was successful and Tnmd was expressed in MC3T3E1 cells and rBMDCs at the same level using CaP and JetPEI.

Based on these results, osteogenesis-related genes were compared between MC3T3E1 and rBMDCs. Runx 2 and SP7 mRNAs were reduced in the JetPEI (Tnmd) group. The released ALP also reduced in the JetPEI (Tnmd) group. This result is similar to that of previous reports that Tnmd overexpression inhibited the expression of osteogenic markers in murine mesenchymal stem cells [27] or adipose-derived stem cells [15]. On the other hand, the expression of these osteogenesis-related genes in the CaP (Tnmd) group was recovered to the level in the untransfected cells. Jeong et al. [28] reported that the release of calcium and phosphorus ions activates the bioactivity of osteoblasts and osteoclasts to accelerate bone regeneration. In this study, the calcium concentration in the supernatant of CaP (Tnmd)-transfected cells was higher than that in JetPEI (Tnmd)-transfected cells; therefore, the calcium concentration in the microenvironment might have an influence on the effect of Tnmd introduction by gene transfection.

Col2α1 and SOX9 play important roles in chondrogenesis; Col2α1, a peculiar regulatory factor of cartilage, is upregulated in proliferating chondrocytes and SOX9 is an indispensable regulator of chondrogenesis [29,30]. In this study, Tnmd expression using JetPEI inhibited chondrogenic activity in MC3T3E1, while that in the CaP (Tnmd) group was not significantly different compared to that of untransfected cells. The effect of Tnmd introduction treatment on chondrogenesis activity might be changed by the presence of calcium ions as in osteogenesis.

In this study, we used type 1 collagen scaffold for the in vivo experiment because numerous collagen-based scaffolds have been used not only for periodontal regeneration therapy [1], but also as a tendon scaffold [31]. Furthermore, a tendon is composed of 60–85% of type I collagen in the total dry weight. The osteogenesis- and chondrogenesis-related gene expression level obtained with JetPEI (EGFP) was the same level obtained with untransfected cells, suggesting that JetPEI loading-mediated enhanced green fluorescent protein has no effects on the osteogenic and chondrogenic activities. Therefore, the JetPEI (EGFP) group was not used in the next in vivo experiment. However, CaP (EGFP) was based on a calcium phosphate nanoparticle and released Ca ions by degradation. Moreover, Ca concentration in the microenvironment affected hard tissue formation; therefore, CaP (EGFP) was set up as a mock for CaP (Tnmd) in an in vivo experiment.

Tnmd-positive cells were observed inside or around the scaffold 28 days after implantation. This indicates that gene transfection using a collagen scaffold, including CaP nanoparticles or cationic reagents, was conducted inside or around the scaffold.

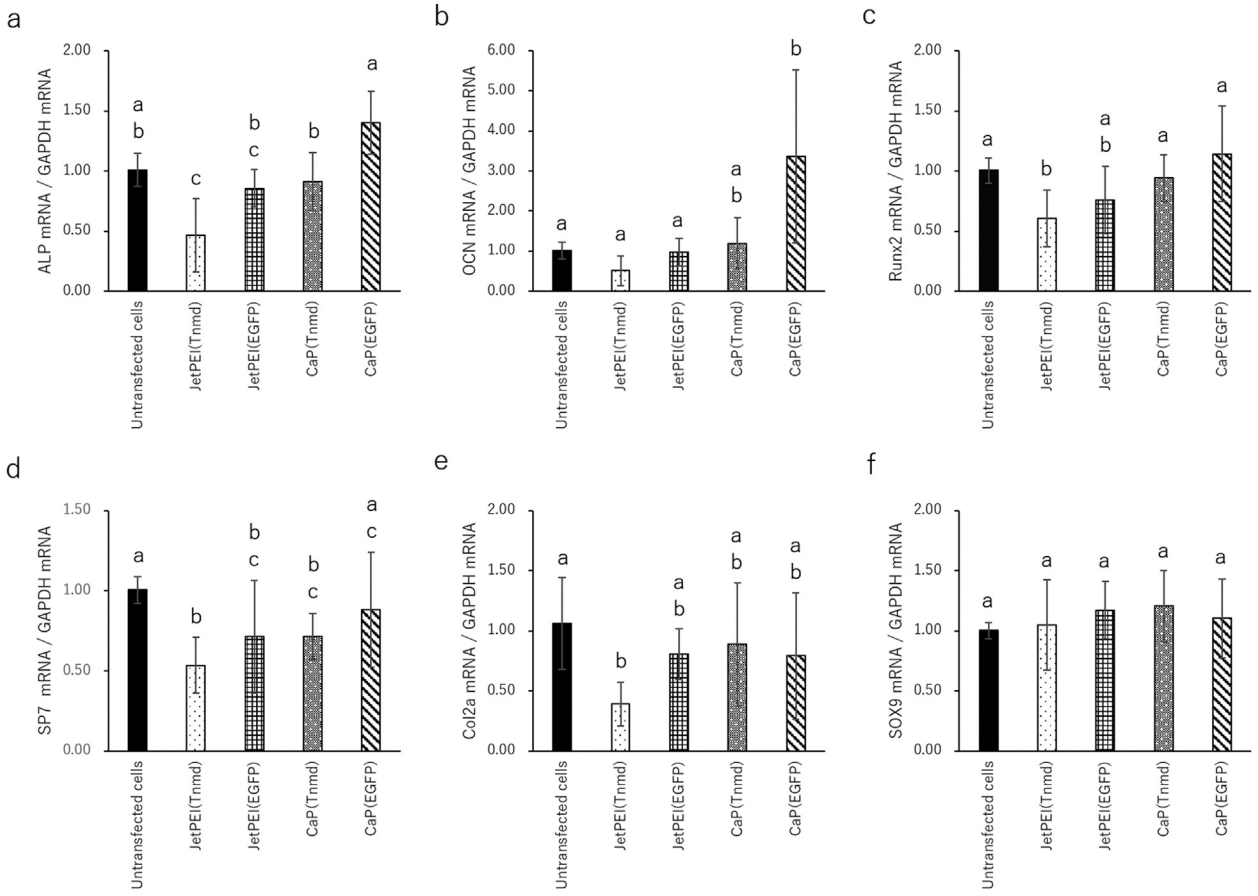

Fig. 3. Gene expression analyses in rBMDCs 3 days after gene transfection. (a) ALP mRNA expression, (b) OCN mRNA expression, (c) Runx 2 mRNA expression, (d) SP7 mRNA expression, (e) Col2α mRNA expression, and (f) SOX9 mRNA expression. Values and error bars indicate the mean and standard deviation, respectively. Significant differences ($p < 0.05$) between groups are denoted by different superscript letters (i.e., bars with the same letter are not significantly different).

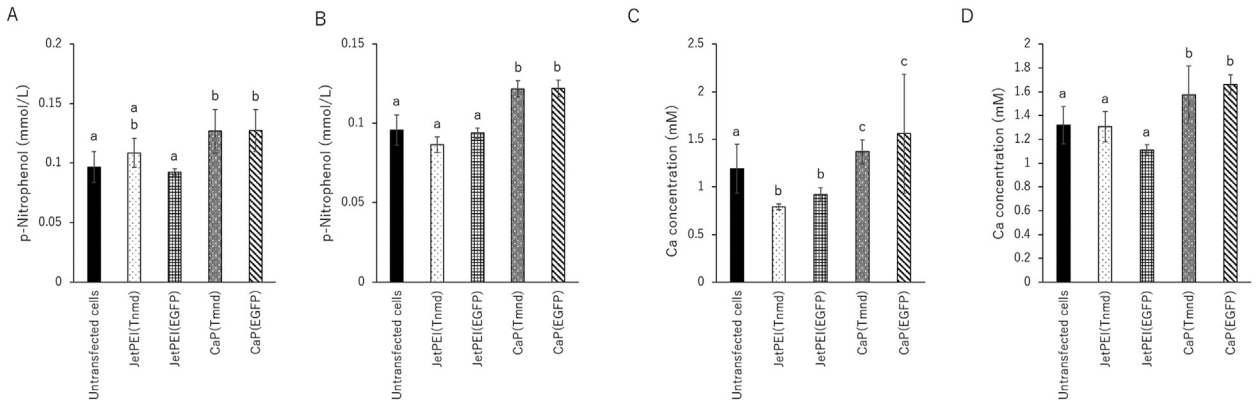

Fig. 4. The concentration of released ALP in the supernatant of the culture medium of MC3T3E1 cells (A) and rBMDCs (B) 3 days after gene transfection. The concentration of released Ca ion in the supernatant of the culture medium of MC3T3E1 cells (C) and rBMDCs (D) 3 days after gene transfection. Values and error bars indicate the mean and standard deviation, respectively. Significant differences ($p < 0.05$) between groups are denoted by different superscript letters (i.e., bars with the same letter are not significantly different).

Table 3
Ratio of Tnmd-stained cells per total cells in an area (371,000 μm^2).

Group	Number of Tnmd staining cells	Tnmd-positive ratio (%) (Stained cells/total cells)
Scaffold alone	27 ± 25^{c}	3 ± 2^{c}
JetPEI (Tnmd)	230 ± 148^{a}	26 ± 9^{a}
CaP (Tnmd)	188 ± 69^{a}	31 ± 17^{a}
CaP (EGFP)	60 ± 34^{b}	7 ± 5^{b}

Parietal bone is formed through intramembranous ossification in embryology; however, Emmett et al. [32] demonstrated that intramembranous ossification and endochondral ossification constructs were observed in bone regeneration treatment using a collagen-based scaffold, including mesenchymal stem cells. From the result of the Elastica Masson staining and toluidine blue staining, the newly formed hard tissue at 28 days after implantation of scaffolds was a mixture of bone-like tissue and cartilage-

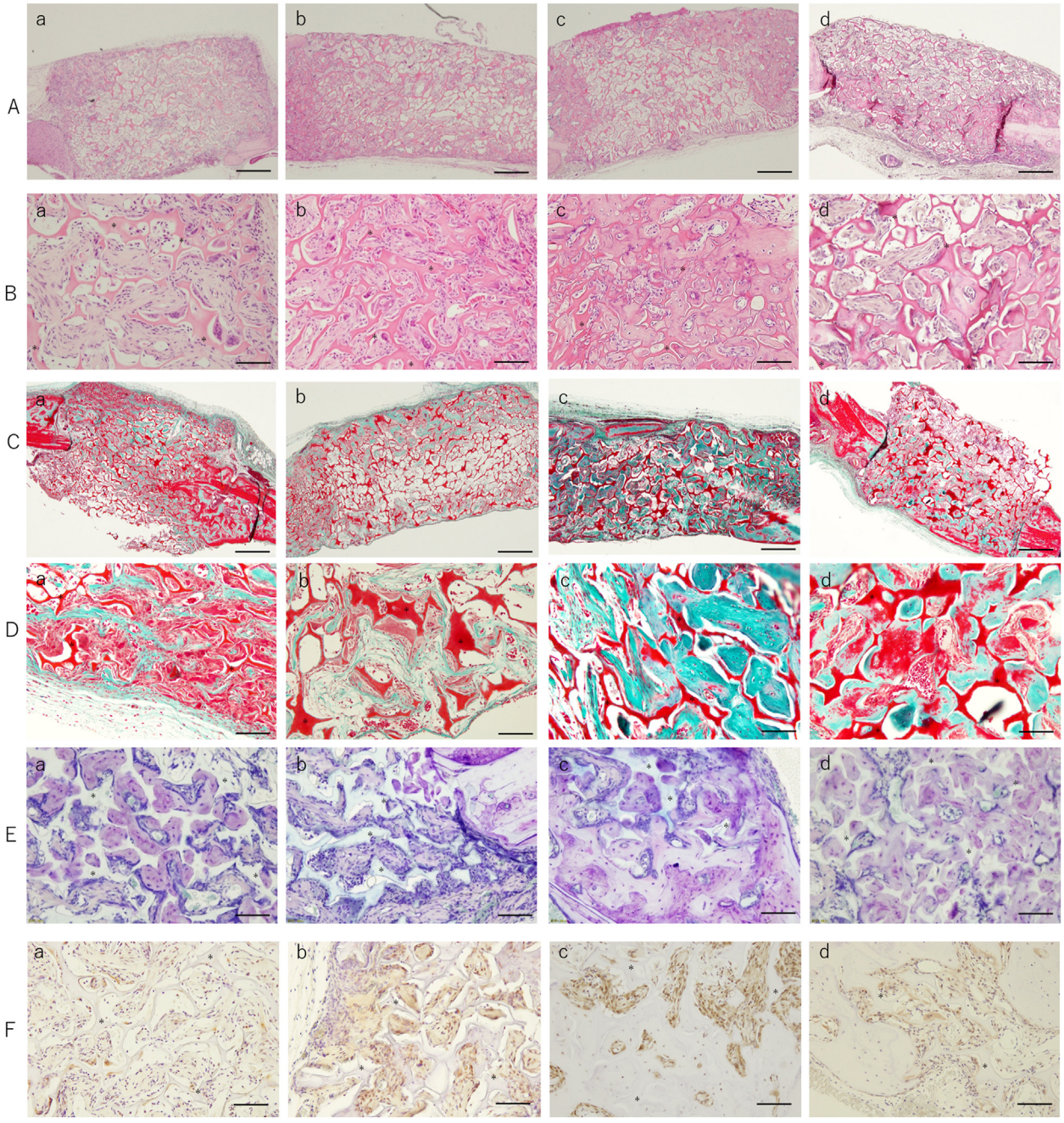

Fig. 5. Histological analysis of cells stained with A: Hematoxylin and eosin (H&E) at low magnification, B: high magnification, C: Elastica Masson at low magnification, D: high magnification, E: Toluidine blue, F: Tnmd at 28 days in the cranium bone defect. (a) Scaffold alone, (b) JetPEI (Tnmd), (c) CaP (Tnmd), (d) CaP (EGFP). The symbol * indicates the remaining collagen fibers. Scale bars: 200 μm in A and C, 100 μm in B, D-F.

like tissue. This tissue construct indicates the bone formation through intramembranous and endochondral ossification. However, collagen fibrils were abundantly observed in the Tnmd expression groups compared to that of the no Tnmd expression groups. Tnmd reportedly promotes cell proliferation and fiber maturation [14,15]. Tnmd-expressing cells might have promoted collagen fiber formation in this study.

From the micro-CT analysis, Tnmd introduction treatment by either non-viral gene transfection vector statistically inhibits the hard tissue formation; however, the remaining bone defect volume of the JetPEI (Tnmd) group was bigger than that of the CaP (Tnmd) group. The amount of Tnmd protein was approximately 9 ng/mL/side in both groups in vivo. At this topical concentration, the effect of Tnmd introduction on bone defects was different from that of the used gene transfection vector. Mutsuzaki et al. [33] reported that a new bone was formed on the implanted tendon scaffold by depositing needle-like low-crystalline apatite on the tendon. Olvera et al. [34] demonstrated that the gene expression of mesenchymal stem cells was changed by the addition of apatite on microfiber scaffolds. The calcium and phosphate ions supplied by the CaP nanoparticles in the atelocollagen scaffold might be efficiently deposited on collagen fibrils, resulting in new hard tissue formation compared to JetPEI (Tnmd). Therefore, the effect of Ca concentration in the localized introduction of

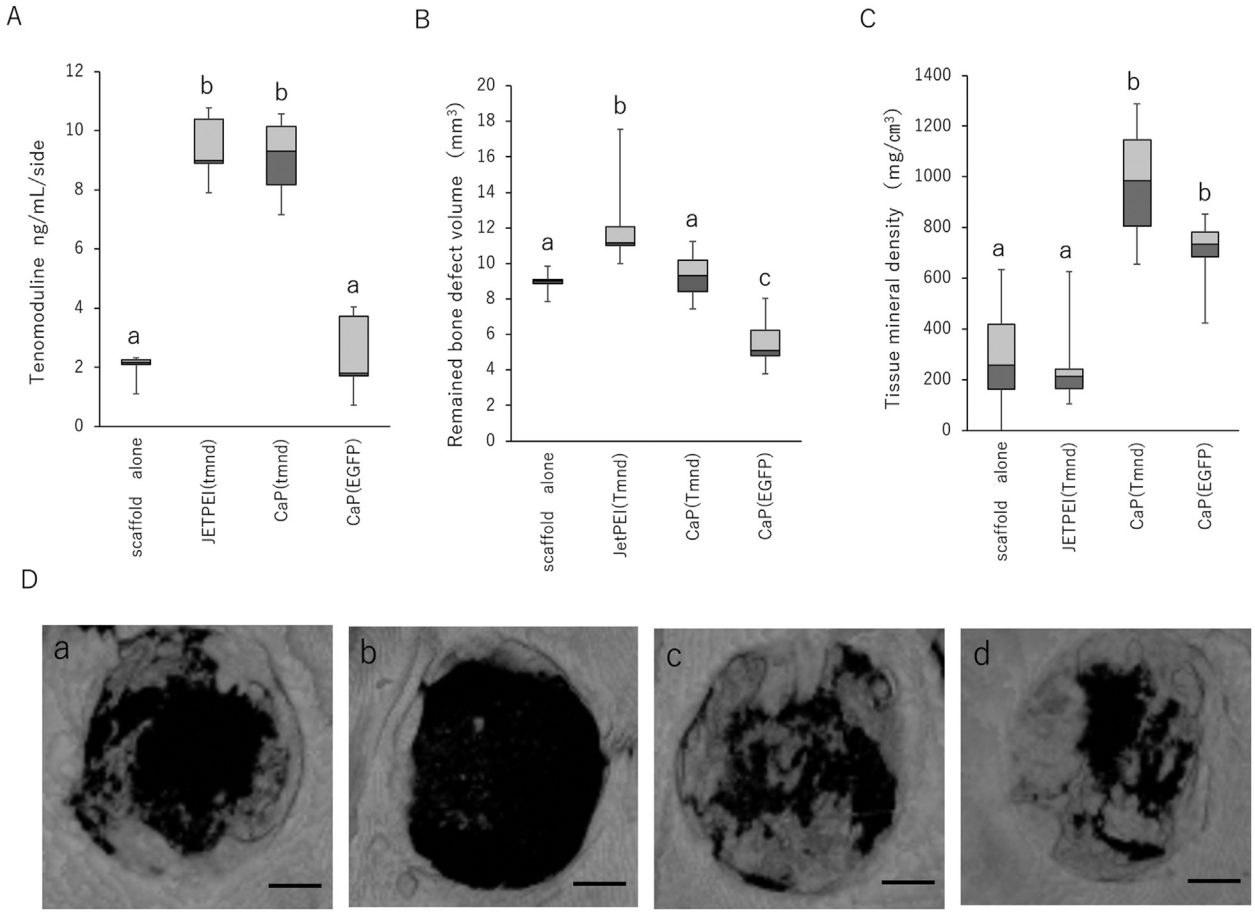

Fig. 6. Comparison of the amount of expressed Tnmd (A) inside the scaffold 28 days after collagen scaffolds, including gene transfection vectors, were implanted. The remaining bone defect volume (B) and tissue mineral density (TMD) (C) determined after micro computed tomography analysis 28 days after implantation, including gene transfection vector, into the cranium bone defect. Values and error bars indicate the mean and standard deviation, respectively. Significant differences ($p < 0.05$) between groups are denoted by different superscript letters (i.e., bars with the same letter are not significantly different). Micro CT images (D) Are shown; scale bars= 1000 μm. (a) Scaffold alone, (b) JetPEI (Tnmd), (c) CaP (Tnmd), (d) CaP (EGFP). The sample number in all groups was ten, as there were ten bone defects.

Tnmd on bone or ligament regeneration should be investigated in the future. In introducing Tnmd introduction treatment for periodontal regeneration therapy, a gene transfection vector might be necessary to distinguish the use depending on the formulation of a collagen fiber part alone or collagen fiber part embedded in hard tissue.

5. Conclusion

In this study, gene transfection using CaP nanoparticles and cationic polyethylenimine derivative reagents was successfully performed in vitro and in vivo. After gene transfection, the calcium concentration in the supernatant was different between the two gene transfection vectors. The effect of Tnmd introduction on hard tissue formation activity was dependent on the gene transfection vectors used. When comparing their expression in untransfected cells, Runx 2, SP7, and SOX9 mRNA expression in MC3T3E1 and ALP, Runx2, and SP7 expression in rBMDCs were reduced by Tnmd introduction treatment when using cationic reagent JetPEI (Tnmd), while that were no statistical difference when using CaP (Tnmd). In the tissue regeneration after Tnmd expression in a rat calvarias bone defect, the remaining bone defect volume in the JetPEI group was bigger than that in the other groups, but was smaller when using CaP (Tnmd), while the amount of Tnmd protein was statistically the same between the JetPEI and CaP nanoparticle groups.

Declaration of competing interest

None.

Acknowledgements

This work was financially supported by a Grant-in-Aid for Scientific Research from theJapan Society for the Promotion of Science, Japan (19K10181). The funders had no role in the study design, data collection and analysis, decision to publish, or manuscript preparation.

References

[1] Chen FM, Jin Y. Periodontal tissue engineering and regeneration: current approaches and expanding opportunities. Tissue Eng B Rev 2010;16:219–55. https://doi.org/10.1089/ten.TEB.2009.0562.
[2] Kinane DF, Berglundh T, Lindhe J, hosts. Parasite interactions in periodontal disease. In: Kinane DF, Berglundh T, Lindhe J, editors. Clinical periodontology and implant dentistry. 4th ed. Oxford: Wiley-Black- well; 2008. p. 150–78.
[3] Liu J, Ruan J, Weir MD, Ren K, Schneider A, Wang P, et al. Periodontal bone-ligament-cementum regeneration via scaffolds and stem cells. Cells 2019;8:537. https://doi.org/10.3390/cells8060537.
[4] Caton JG, DeFuria EL, Polson AM, Nyman S. Periodontal regeneration via selective cell repopulation. J Periodontol 1987;58:546–52. https://doi.org/10.1902/jop.1987.58.8.546.
[5] Kato A, Miyaji H, Kosen Y, Yokoyama H, Ishizuka R, Tokunaga K, et al. Periodontal healing by implantation of collagen hydrogel-sponge

composite in one-wall infrabony defects in beagle dogs. J Oral Tissue Eng 2010;8:39–46.
[6] Andersson L, Malmgren B. The problem of dentoalveolar ankylosis and subsequent replacement resorption in the growing patient. Aust Endod J 1999;25:57–61. https://doi.org/10.1111/j.1747-4477.1999.tb00088.x.
[7] Brandau O, Meindl A, Fässler R, Aszódi A. Fa ssler R, Aszo'di AA. novel gene, tendin, is strongly expressed in tendons and ligaments and shows high homology with chondromodulin-I. Dev Dynam 2001;221:72–80. https://doi.org/10.1002/dvdy.1126.
[8] Shukunami C, Oshima Y, Hiraki Y. Molecular cloning of tenomodulin, a novel chondromodulin-I related gene. Biochem Biophys Res Commun 2001;280:1323–7. https://doi.org/10.1006/bbrc.2001.4271.
[9] Itaya T, Kagami H, Okada K, Yamawaki A, Narita Y, Inoue M, et al. Characteristic changes of periodontal ligament-derived cells during passage. J Periodontal Res 2009;44:425–33. https://doi.org/10.1111/j.1600-0765.2008.01137.x.
[10] Shukunami C, Takimoto A, Oro M, Hiraki Y. Scleraxis positively regulates the expression of tenomodulin, a differentiation marker of tenocytes. Dev Biol 2006;298:234–47. https://doi.org/10.1016/j.ydbio.2006.06.036.
[11] Oshima Y, Shukunami C, Honda J, Nishida K, Tashiro F, Miyazaki J, et al. Expression and localization of tenomodulin, a transmembrane type chondromodulin-I-related angiogenesis inhibitor, in mouse eyes. Invest Ophthalmol Vis Sci 2003;44:1814–23. https://doi.org/10.1167/iovs.02-0664.
[12] Wang W, Liu GX, Li YH, Li XD, He Y. Inhibitory effect of tenomodulin versus ranibizumab on *in vitro* angiogenesis. Int J Ophthalmol 2017;10:1212–6. https://doi.org/10.18240/ijo.2017.08.04.
[13] Docheva D, Hunziker EB, Fässler R, Brandau O. Tenomodulin is necessary for tenocyte proliferation and tendon maturation. Mol Cell Biol 2005;25:699–705. https://doi.org/10.1128/MCB.25.2.699-705.2005.
[14] Komiyama Y, Ohba S, Shimohata N, Nakajima K, Hojo H, Yano F, et al. Tenomodulin expression in the periodontal ligament enhances cellular adhesion. PLoS One 2013;8. https://doi.org/10.1371/journal.pone.0060203. https://doi:10.1371/journal.pone.0060203:e60203.
[15] Shi Y, Xiong Y, Jiang Y, Zhang Z, Zhou G, Zhang W, et al. Conditional tenomodulin overexpression favors tenogenic lineage differentiation of transgenic mouse derived cells. Gene 2017;598:9–19. https://doi.org/10.1016/j.gene.2016.10.028.
[16] Percival CJ, Richtsmeier JT. Angiogenesis and intramembranous osteogenesis. Dev Dynam 2013;242:909–22. https://doi.org/10.1002/dvdy.23992.
[17] Lin D, Alberton P, Delgado Caceres M, Prein C, Clausen-Schaumann H, Dong J, et al. Loss of tenomodulin expression is a risk factor for age-related intervertebral disc degeneration. Aging Cell 2020;19:e13091. https://doi.org/10.1111/acel.13091.
[18] Sokolova VV, Radtke I, Heumann R, Epple M. Effective transfection of cells with multi-shell calcium phosphate-DNA nanoparticles. Biomaterials 2006;27:3147–53. https://doi.org/10.1016/j.biomaterials.2005.12.030.
[19] Tenkumo T, Rotan O, Sokolova V, Epple M. Protamine increases transfection efficiency and cell viability after transfection with calcium phosphate nanoparticles. Nano Biomed 2013;5:64–74.
[20] Xiang C, Tenkumo T, Ogawa T, Kanda Y, Nakamura K, Shirato M, et al. Gene transfection achieved by utilizing antibacterial calcium phosphate nanoparticles for enhanced regenerative therapy. Acta Biomater 2021;119:375–89. https://doi.org/10.1016/j.actbio.2020.11.003.
[21] Vanegas Sáenz JR, Tenkumo T, Kamano Y, Egusa H, Sasaki K. Amiloride-enhanced gene transfection of octa-arginine functionalized calcium phosphate nanoparticles. PLoS One 2017;12:e0188347. https://doi.org/10.1371/journal.pone.0188347.
[22] Sokolova V, Knuschke T, Buer J, Westendorf AM, Epple M. Quantitative determination of the composition of multi-shell calcium phosphate-oligonucleotide nanoparticles and their application for the activation of dendritic cells. Acta Biomater 2011;7:4029–36. https://doi.org/10.1016/j.actbio.2011.07.010.
[23] Herz J, Gerard RD. Adenovirus mediated transfer of low density lipoprotein receptor gene acutely accelerates cholesterol clearance in normal mice. Proc Natl Acad Sci U S A 1993;90:2812–6. https://doi.org/10.1073/pnas.90.7.2812.
[24] Simon RH, Engelhardt JF, Yang Y, Zepeda M, Weber-Pendleton S, Grossman M, et al. Adenovirus mediated transfer of the CFTR gene to lung of nonhuman primates: toxicity study. Hum Gene Ther 1993;4:771–80. https://doi.org/10.1089/hum.1993.4.6-771.
[25] Walther W, Stein U. Viral vectors for gene transfer: a review of their use in the treatment of human diseases. Drugs 2000;60:249–71. https://doi.org/10.2165/00003495-200060020-00002.
[26] Sokolova V, Epple M. Biological and medical applications of calcium phosphate nanoparticles. Chemistry 2021;27:7471–88. https://doi.org/10.1002/chem.202005257.
[27] Jiang Y, Shi Y, He J, Zhang Z, Zhou G, Zhang W, et al. Enhanced tenogenic differentiation and tendon-like tissue formation by tenomodulin overexpression in murine mesenchymal stem cells. J Tissue Eng Regen Med 2017;11:2525–36. https://doi.org/10.1002/term.2150.
[28] Jeong J, Kim JH, Shim JH, Hwang NS, Heo CY. Bioactive calcium phosphate materials and applications in bone regeneration. Biomater Res 2019;23:4. https://doi.org/10.1186/s40824-018-0149-3.
[29] Bell DM, Leung KK, Wheatley SC, Ng LJ, Zhou S, Ling KW, et al. SOX9 directly regulates the type-ll collagen gene. Nat Genet 1997;16:174–8. https://doi.org/10.1038/ng0697-174.
[30] Ng LJ, Wheatley S, Muscat GE, Conway-Campbell J, Bowles J, Wright E, et al. SOX9 binds DNA, activates transcription, and coexpresseswith type II collagen during chondrogenesis in the mouse. Dev Biol 1997;183:108–21. https://doi.org/10.1006/dbio.1996.8487.
[31] Jaiswal D, Yousman L, Neary M, Fernschild E, Zolnoski B, Katebifar S, et al. Tendon tissue engineering: biomechanical considerations. Biomed Mater 2020;15:052001. https://doi.org/10.1088/1748-605X/ab852f.
[32] Thompson EM, Matsiko A, Kelly DJ, Gleeson JP, O'Brien FJ. An endochondral ossification-based approach to bone repair: chondrogenically primed mesenchymal stem cell-laden scaffolds support greater repair of critical-sized cranial defects than osteogenically stimulated constructs in vivo. Tissue Eng 2016;22:556–67. https://doi.org/10.1089/ten.TEA.2015.0457.
[33] Mutsuzaki H, Sakane M, Ito A, Nakajima H, Hattori S, Miyanaga Y, et al. The interaction between osteoclast-like cells and osteoblasts mediated by nanophase calcium phosphate-hybridized tendons. Biomaterials 2005;26:1027–34. https://doi.org/10.1016/j.biomaterials.2004.03.039.
[34] Olvera D, Sathy BN, Kelly DJ. Spatial presentation of tissue-specific extracellular matrix components along electrospun scaffolds for tissue engineering the bone-ligament interface. ACS Biomater Sci Eng 2020;6:5145–61. https://doi.org/10.1021/acsbiomaterials.0c00337.